Received: 8 September 2019 | Accepted: 13 November 2019 | Published on: 27 February 2020

DOI: 10.1002/asna.202023772

Astronomische Nachrichten

ORIGINAL ARTICLE

Supernova remnants in nearby galaxies

Manami Sasaki

Dr. Karl Remeis Sternwarte & Erlangen Center for Astroparticle Physics, Friedrich Alexander Universität Erlangen-Nürnberg, Bamberg, Germany

Correspondence
Manami Sasaki, Dr. Karl Remeis Sternwarte & Erlangen Center for Astroparticle Physics, Friedrich Alexander Universität Erlangen-Nürnberg, Bamberg, Germany.
Email: manami.sasaki@fau.de

Funding information
Deutsche Forschungsgemeinschaft, Grant/Award Number: SA 2131/5-1 and 12-1

Abstract

Supernova remnants (SNRs) are the aftermath of stellar explosions, which inject large amounts of energy into the interstellar medium (ISM), carving out new structures and transferring kinetic energy to the ISM. They also act as recycling centers, which return elements processed in stars to the ISM, and cosmic particle accelerators. The evolution of SNRs can be best studied in soft X-ray line and continuum emission, since they mainly consist of very hot plasma (10^6–10^7 K). While it is difficult to observe these soft X-ray sources in our own Galaxy due to absorption by matter in the Galactic plane, the Magellanic Clouds as well as the nearby spiral galaxies M 31 and M 33 are ideal targets to study both particular SNRs in detail and the SNR population in a galaxy as a whole. Various studies of SNRs in the Local Group galaxies have been carried out with XMM-Newton or Chandra since the launch of the mission, and in the coming years the new X-ray all-sky survey performed with eROSITA will provide us with more complete data of SNRs in the nearby Universe to low flux limits.

KEYWORDS

supernova remnants, milky way, magellanic clouds, local group

1 INTRODUCTION

When a star dies in a supernova explosion, strong shock waves are formed. They create objects called supernova remnants (SNRs), which are responsible for ionizing, heating, and forming new structures in the interstellar medium (ISM) of a galaxy. Particles gain relativistic energies in the shocks of SNRs and become galactic cosmic rays. New heavier elements, which were formed in the progenitor star or in the explosion, are expelled into the environment. Therefore, SNRs are a crucial piece in the galactic matter cycle.

In supernovae, a large amount of energy is released, which is transferred to the debris of the star and its surroundings. Stellar matter is thrown out with an initial velocity of $\sim$10,000 km s^{-1}, and a spherical blast shock wave expands into the ISM. After the blast wave has swept up as much mass as the ejecta mass, the pressure difference between the shocked ISM and the hot ejecta drives a second shock wave back into the interior of the SNR, which is called the reverse shock. Both the shocked ISM and the ejecta are thus heated to X-ray emitting temperatures.

There are currently about 300 identified SNRs in our Galaxy (Green 2019). Most of the known SNRs are found in the direction of the Galactic center region, and are thus heavily affected by interstellar absorption. The first extragalactic SNRs were identified in the star-forming satellite galaxies of the Milky Way and the Magellanic Clouds in the 1960s and 1970s in radio and optical observations (Davies et al. 1976; Mathewson & Clarke 1973; Mathewson

TABLE 1 Number of SNRs in nearby galaxies

	Distance (kpc)	Number of SNRs and candidates	References[a]
LMC	50	59	[1], [2]
SMC	60	24	[3], [4]
M 31	750	156	[5], [6]
M 33	800	217	[7], [8]
M 83	46,000	~250	[9], [10]

[a] [1] Maggi et al. (2016), [2] Bozzetto et al. (2017), [3] Badenes et al. (2010), [4] Haberl et al. (2012a), [5] Sasaki et al. (2012), [6] Lee & Lee (2014a), [7] Long et al. (2010), [8] White et al. (2019), [9] Long et al. (2014), [10] Blair et al. (2015).

& Healey 1963; Westerlund & Mathewson 1966). Table 1 summarizes the number of identified SNRs in the Large and Small Magellanic Clouds (LMC, SMC) and the two other spiral galaxies in the Local Group M 31 and M 33, as well as the nearby star-burst galaxy M 83.

1.1 | X-ray Observations

In the forward blast wave shock and the reverse shock in SNRs, the ISM and the SNR ejecta are heated to temperatures of $\sim 10^6$ K. Therefore, SNRs are bright X-ray sources with soft thermal X-ray emission. In addition, in some young SNRs the particle acceleration is sufficiently strong to cause significant synchrotron emission from non-thermal electrons (see, e.g., Vink 2012, for a review). The morphology of SNRs will be affected both by the explosion and the interaction with the ambient medium.

Combined imaging and spectral analyses will reveal the distribution and composition of the ejecta, from which the distribution and abundances of elements forged inside the progenitor and the supernova explosion can be derived. The elements in the ejecta can reveal whether the supernova was caused by core collapse of a massive star or by the thermonuclear explosion of a white dwarf. The X-ray spectrum consists of contributions to the continuum from free–free emission, recombination, and two-photon emission. There is also ample line emission from electron–ion collisions or recombination. In some cases, we will also observe continuum emission from non-thermal electrons. Therefore, in X-rays, the properties of the shock, the shocked ISM, and the ejecta of the supernova explosion can be studied.

1.2 | Multi-wavelength Observations

In addition, multi-wavelength comparison is crucial for the understanding of the physics of SNRs. While X-ray synchrotron emitting electrons have higher energies (TeV) and thus short life times, electrons emitting radio synchrotron emission have lower energies (GeV) and will radiate for a longer time (~100,000 years), which is comparable with or longer than the age of the SNR. Therefore, most of the SNRs have been detected as bright radio sources. For the flux density of synchrotron emission from non-thermal electrons, we typically find $S \propto \nu^{-\alpha}$ for frequency ν with $\alpha \approx 0.5$.

In the optical spectrum, the shocks of SNRs can be observed in Hα emission. In addition, radiative shocks in denser ISM will cause emission of optical forbidden lines from different ionization states such as [O III] $\lambda\lambda$ 4959, 5007, [O I] $\lambda\lambda$ 6300, 6363, [N II] $\lambda\lambda$ 6549, 6583, and [S II] $\lambda\lambda$ 6717, 6731 (Fesen et al. 1985, and references therein).

Radiative shock of SNRs propagating into the ambient ISM will also cause [Fe II] $\lambda\lambda$ 1.27, 1.64 μm emission, which is observed in the infrared (IR, Oliva et al. 1989, and references therein). Most of the IR emission observed from SNRs has its origin in thermal dust, which is one of the major components of the ISM, next to atomic and molecular gas, clouds, and plasma. In SNRs, interstellar dust can be heated by radiation of the hot interior shocked plasma and by collisions caused by the shock. Dust is also produced in supernova ejecta and is released into the ISM in SNRs. Therefore, IR emission of heated dust is also often observed from SNRs.

At the highest energies, emission from radioactive decay of elements produced in the supernova explosion (Iyudin et al. 1994; Mochizuki et al. 1999, and references therein) as well as emission from highly relativistic cosmic rays will be observed in the γ-ray regime.

Multi-frequency studies of SNRs from the radio all the way up to γ-ray regime help understand the explosion mechanisms, physics of interstellar shocks, heating of the surrounding material, distribution of chemically enriched material that was processed in stellar interior and was expelled by the supernova explosion, and the properties of the interstellar environment in which the shock is expanding.

2 | THE MAGELLANIC CLOUDS

SNRs are typically soft X-ray sources due to their hot interior. Because of the high absorption in the Galactic plane, these soft and extended X-ray sources can be observed only in a small portion of our own Galaxy. The largest and actively star-forming satellite galaxies of the Milky Way, the Large and Small Magellanic Clouds (LMC, SMC), with their low foreground absorption and small distances of ~50 and 62 kpc, respectively (Graczyk et al. 2014; van den Bergh 1999), offer an ideal laboratory for the

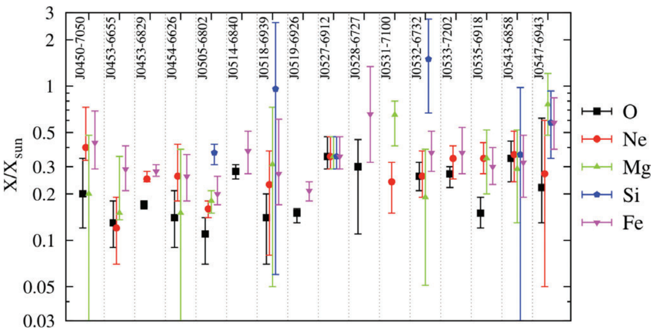

FIGURE 1 Element abundances in the LMC ISM, relative to the solar values, derived from the XMM-Newton spectrum of LMC SNRs (taken from Maggi et al. 2016)

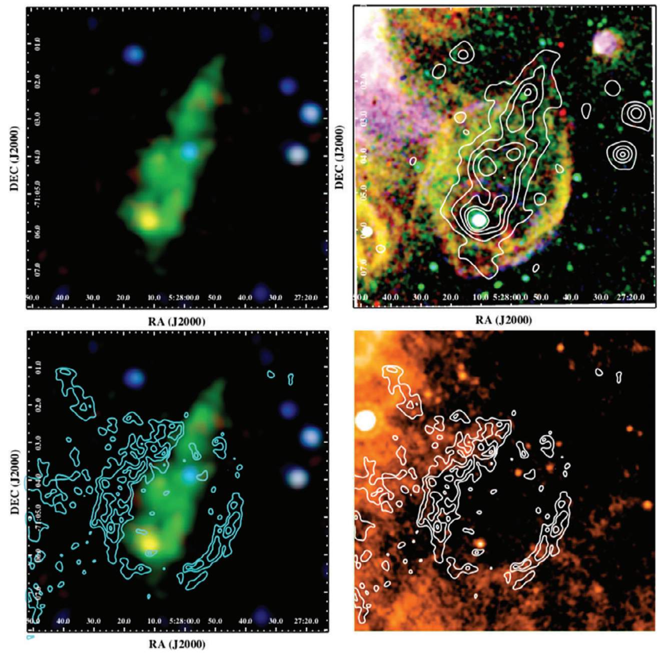

FIGURE 2 *Top left*: XMM-Newton EPIC image of LMC SNR J0527-7104 in false color, with red, green, and blue corresponding to 0.3–0.7, 0.7–1.1, and 1.1–4.2 keV, respectively. *Top right*: continuum subtracted Magellanic Cloud Emission Line Survey (MCELS) image of the same area of the sky with Hα in red, [S II] in green, and [O III] in blue, overlaid with 0.7–1.1 keV contours. *Bottom left*: same as top left but with [S II]/Hα contours with the lowest level corresponding to [S II]/Hα = 0.67. *Bottom right*: Spitzer MIPS 24-μm image with [S II]/Hα contours. Taken from Kavanagh et al. (2016)

study of the complete sample of SNRs in galaxies. Their proximity enables spatially resolved studies of the SNRs, and their accurately known distances permit the analysis of the energetics of each SNR. In addition, the wealth of wide-field multi-wavelength data available from radio, sub-mm, infrared, to optical emission-line images provides crucial information about the environments in which these SNRs are born and evolve. Observations of the LMC and the SMC allow us to study not only the global properties of SNRs in a galaxy but also specific sub-classes in detail (e.g., sorted by X-ray and radio morphology, diameter, or progenitor supernova type).

2.1 | SNR population in the Magellanic Clouds

Therefore, we have been carrying out systematic studies of SNRs in the MC since the launch of XMM-Newton using additional optical and radio data. We have thus been also engaged in a very successful project to observe SNR candidates identified with ROSAT detections from Kahabka et al. (1999), and Haberl & Pietsch (1999). We have obtained data of the main parts of the SMC and a large fraction of the optical bright part of the LMC in large programs and dedicated observations of selected SNR candidates. There are 59 confirmed SNRs in the LMC and 19 in the SMC at present, and many more candidates. We have performed an extensive study of the known population to date (Maggi et al. 2016 and Maggi et al. 2019 for the LMC and the SMC, respectively) in the X-ray and also in the radio band (Bozzetto et al. 2017). These global studies of the SNR population allow us to compare morphologies or element distribution for a large sample of SNRs and compile an evolution sequence of SNRs. Furthermore, we have derived interstellar element abundances from the X-ray spectra of shell-type SNRs in the LMC (Figure 1, Maggi et al. 2016).

2.2 | New supernova remnants

In order to improve our understanding of the physics of SNR shocks and the interaction of SNRs with the ambient multi-phase ISM, we also have considered selected SNRs and carried out detailed multi-wavelength studies (e.g.,Kavanagh et al. 2013, 2015, 2016; Maggi et al. 2014; Sasaki et al. 2006).

In particular, we have discovered several SNRs that are bright in their interiors in a narrow energy range of ~1 keV. This is due to the enhanced Fe L-shell emission inside the shell, indicating that the SNR was formed by a type Ia supernova. The SNR with the most intriguing morphology of the interior emission with very faint softer shell emission is SNR J0527-7104, shown in Figure 2 (Kavanagh et al. 2016).

2.3 | Composite supernova remnants

Observations with XMM-Newton have also allowed us to resolve and identify new pulsar wind nebulae (PWNe) and X-ray binaries in SNRs in the MC.

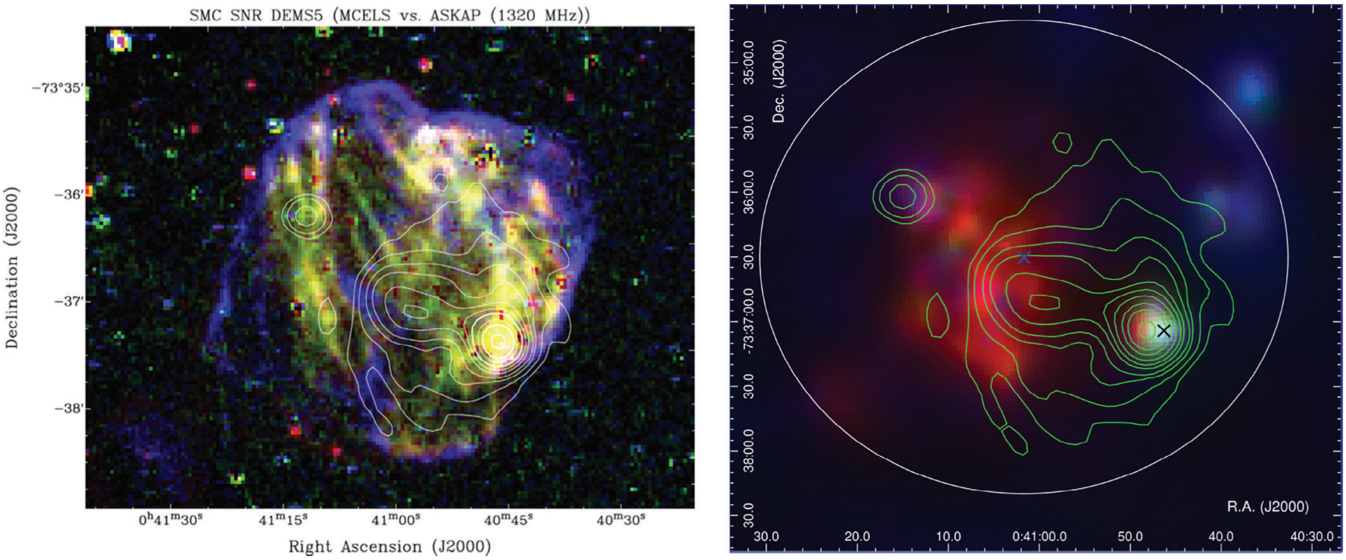

FIGURE 3 MCELS (*left*, *red*: Hα, green: [S II], *blue*: [O III]) and XMM-Newton EPIC (*right*, *red*: 0.2–1 keV, green: 1–2 keV, *blue*: 2–4.5 keV) images of the SMC SNR DEM S5 with contours of the 1320 MHz radio continuum (Alsaberi et al. 2019). In X-rays there is a soft shell emission and a harder point source which coincides with the head of the bow-shock PWN seen in radio. The cross marks the position of the hard X-ray point source

There are three known composite SNRs with a thermal shell and a PWN observed in X-rays in the LMC (SNR N206, J0540-6919 [N158A], and J0453-6829) and one in the SMC (SNR IKT 16). In addition, we have discovered a pulsar-powered bow-shock nebula in the SMC SNR DEM S5 (Alsaberi et al. 2019). This SNR is bright in the optical spectrum and show filamentary structures in the shell (Figure 3, left). The XMM-Newton data show diffuse soft X-ray emission (Figure 3, right) and a hard X-ray source with extended emission around it, west of the main X-ray emission, which coincides with a pulsar, and a bow-shock nebula detected in the radio band.

Interestingly, there have also been detections of high-mass X-ray binaries (HMXBs) inside SNRs: CXOU 053600.0-673507 in the SNR 0535-67.5 in the HII region DEM L241 in the LMC (Seward et al. 2012), as well as in SXP 1062 (see Figure 4; Haberl et al. 2012b) and in SXP 1323 (Gvaramadze et al. 2019) in the SMC. While DEM L241 was known to be an SNR and the HMXB was discovered later, in the two SMC cases the emission from the HMXB dominates the SNR emission, and the surrounding shell was later found in newer observations. Finding HMXBs in SNRs is of particular interest since the SNR can give information about the possible progenitor and hence about the formation mechanisms of a neutron star or a black hole.

3 | M 31 AND M 33

The spiral galaxies in the Local Group, i.e., the Milky Way, M 31, and M 33, are the best studied normal galaxies. In the galaxies M 31 and M 33, we are able to detect fainter objects than in any other galaxy outside the Local Group and determine their relation to other components in the galaxy. Since SNRs predominantly emit soft X-rays, they are ideal targets for XMM-Newton. We have studied the SNR population in M 31 (Sasaki et al. 2012, 2018) using the data of the XMM-Newton survey of M 31 (Stiele et al. 2011), the *XMM-Newton* large program on the northern disk of M 31, and the Hα [S II] and [O III] emission line images as well as the *UBVRI* band images of the Local Group galaxy survey (Massey et al. 2002) in the optical band. A recent X-ray study of the SNR population in M 33 has been performed by Garofali et al. (2017) based on an XMM-Newton survey. The comparison of the catalogs of X-ray SNRs to those of SNRs detected in the optical band in M 31 and M 33 (Lee & Lee 2014a 2014b, respectively) has shown that only a small fraction of optically detected SNRs are also X-ray sources, and vice versa. In these galaxies, SNRs have been detected in X-rays down to luminosities of $\lesssim 10^{35}$ erg s^{-1} with XMM-Newton (0.3–10.0 keV).

4 | POPULATIONS OF SUPERNOVA REMNANTS

The Magellanic Clouds, M 31, and M 33 have very different dominating interstellar structures, metallicities, stellar populations, and star-formation rates, making differences in their ensemble of X-ray SNRs that are of great interest for testing theories for the dominant SNR and ISM characteristics that affect SNR X-ray emission.

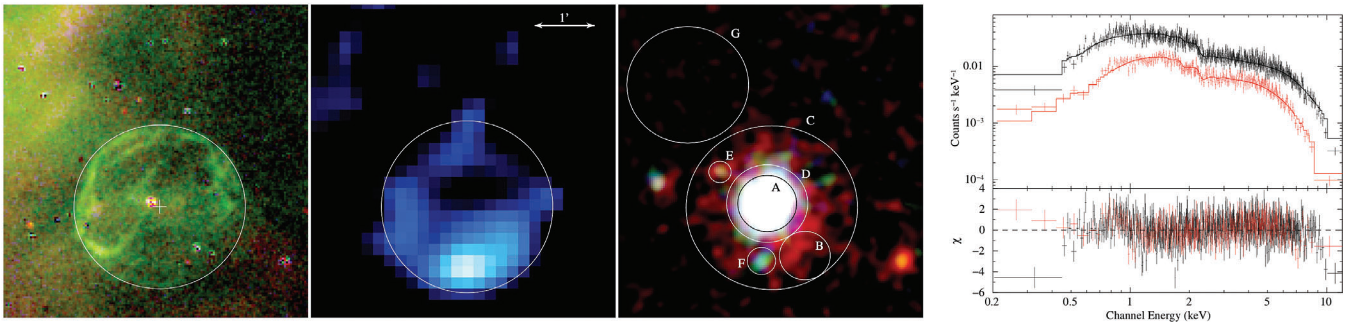

FIGURE 4 *Left panel*: Images of SNR around the SMC HMXB SXP 1062 from MCELS (*left*, *red*: Hα, green: [O III], blue: [S II]), MOST 36 cm (middle), and XMM-Newton (right, 0.2–1.0, 1.0–2.0, and 2.0–4.5 keV in red, green, and blue, respectively). The large white circle shows the extent of the SNR derived from the optical image, the cross is the geometric center of the circle. The smaller circles in the right image indicate the extraction regions for the spectral analysis. *Right panel*: XMM-Newton EPIC pn (black) and MOS2 (red) spectrum of the SNR around the HMXB SXP 1062 (Haberl, Sturm, Filipović, et al., 2012)

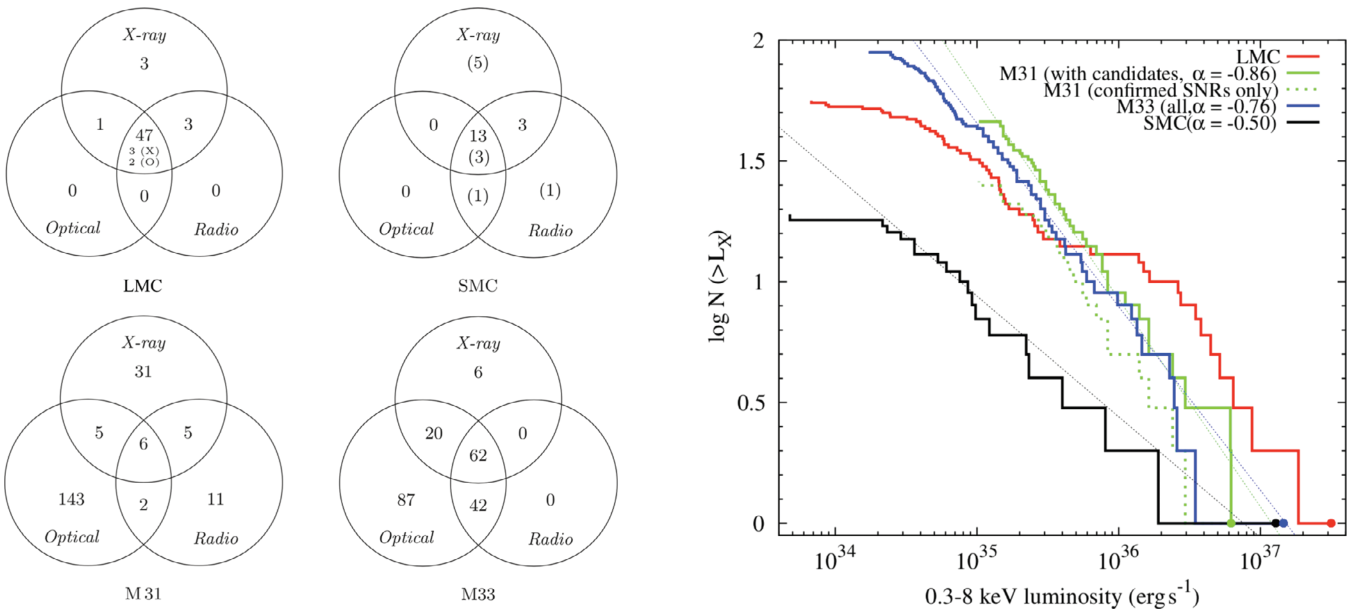

FIGURE 5 *Left*: Venn diagrams showing the number of X-ray, optical, and radio SNRs in LMC, SMC, M 31, and M 33. In the upper left diagram, (X) or (O) denotes objects with emission in these bands but without significant detections (X-ray or optical, respectively). In the upper right diagram, numbers of SNR candidates are given in parentheses. Taken from Bozzetto et al. (2017). *Right*: X-ray luminosity functions (XLFs) of SNRs. Thick lines are used for the observed XLFs. The thin dotted lines show the power-law fit ($N(> L_X) \propto L_X^{\alpha}$) to the XLFs. Taken from Maggi et al. (2016)

Figure 5 (left, Bozzetto et al. 2017) shows Venn diagrams of the number of SNRs detected in different wavelength bands. Typically, SNRs are bright radio and X-ray sources due to their shocks. In addition, optical emission can be observed when the shock is radiative or is expanding into dense parts of the ISM. Since the shock produces hot interior plasma that emits X-ray emission, all known SNRs in the Magellanic Clouds are detected in X-rays, and the majority is also detected in radio and optical bands. On the contrary, in M 31 and M 33, a large number of SNRs are detected in the optical band, and a large fraction has no detections in radio or X-ray band. In distant galaxies, it seems that it is more difficult to detect X-ray SNRs due to absorption, while radio SNRs are easily confused with HII regions. The non-detection of SNRs in X-rays due to absorption is also observed in the Milky Way, in which most of the known SNRs are detected in the radio band.

A very powerful way to study populations of a certain class of objects in different galaxies is to look at their luminosity functions. In Figure 5 (right, Maggi et al. 2016) one can see that the cumulative luminosity function of SNRs in the SMC and the LMC is much flatter than those in M 33 or M 31. In particular, the LMC hosts very bright SNRs. This difference is most likely caused by the lower metallicities in the Magellanic Clouds than in the spiral galaxies and possibly by the difference in ISM density in which the SNRs are expanding.

5 | SUMMARY AND OUTLOOK

Building upon the results of the early X-ray missions ROSAT or the Einstein Observatory, we have been carrying out systematic study of the populations of SNRs in nearby galaxies since the launch of XMM-Newton and the Chandra X-ray Observatory. X-ray observations of SNRs combined with multi-wavelength studies can reveal

- the type of SN explosion and structure and abundances in the ejecta,
- temperature, ionization, density distributions, and element abundances in the surrounding ISM,
- mass loss history of the progenitor,
- time since the explosion, and
- presence or absence of a neutron star and its environment.

The observed emission of SNRs also depends on external factors. In X-rays, it is mainly affected by absorption, which makes a global study of the SNR population in our Galaxy impossible. Furthermore, the relatively large variation in distance makes an accurate study of size or energetics difficult. SNR populations in other galaxies are not affected by these external factors and can provide us with information about the stellar evolution and supernova explosion mechanisms, the ISM, and, in particular, the metallicity, the underlying stellar population, and the star-formation history of the galaxy.

With the new X-ray telescope eROSITA, which was successfully launched on July 13, 2019 onboard the Spektr-RG satellite, we will obtain new data of the entire X-ray sky with a sensitivity 20–30 times that of the ROSAT all-sky survey in the soft X-ray band (Merloni et al. 2012). Therefore, the eROSITA all-sky survey (eRASS) is perfect for studies of both thermal and non-thermal SNRs in the Milky Way and nearby galaxies. We will use eRASS to confirm and to study new SNRs in our Galaxy with unprecedented grasp (field-of-view times effective area), in particular those with non-thermal (synchrotron) X-ray emission, and to obtain a census of the SNR population in the MC and to perform a statistical study of their physical properties, progenitors, environments, and their impact on the ISM, star formation, and cosmic ray population in the galaxies. The full coverage of the nearby galaxies with homogeneous flux limits is crucial for a study of the entire population of SNRs and their relation and consequences on the evolution of galaxies.

ACKNOWLEDGMENT

The author acknowledges support by the Deutsche Forschungsgemeinschaft through the Heisenberg professor grants SA 2131/5-1 and 12-1.

REFERENCES

Alsaberi, R. Z. E., Maitra, C., Filipović, M. D., et al. 2019, *MNRAS*, *486*(2), 2507. https://doi.org/10.1093/mnras/stz971.

Badenes, C., Maoz, D., & Draine, B. T. 2010, *MNRAS*, *407*, 1301. https://doi.org/10.1111/j.1365-2966.2010.17023.x.

van den Bergh, S. 1999, The Magellanic Clouds, Past, Present and Future - A Summary of IAU Symposium No. 190. in *IAU Symp. 190: New Views of the Magellanic Clouds* Vol. 190, p. 569. Retrieved from http://adsabs.harvard.edu/cgi-bin/nph-bib_query?bibcode=1999IAUS..190..569V&db_key=AST

Blair, W. P., Winkler, P. F., Long, K. S., et al. 2015, *ApJ*, *800*(2), 118. https://doi.org/10.1088/0004-637X/800/2/118.

Bozzetto, L. M., Filipović, M. D., Vukotić, B., et al. 2017, *ApJS*, *230*, 2. https://doi.org/10.3847/1538-4365/aa653c.

Davies, R. D., Elliott, K. H., & Meaburn, J. 1976, *MmRAS*, *81*, 89.

Fesen, R. A., Blair, W. P., & Kirshner, R. P. 1985, *ApJ*, *292*, 29. https://doi.org/10.1086/163130.

Garofali, K., Williams, B. F., Plucinsky, P. P., et al. 2017, *MNRAS*, *472*(1), 308. https://doi.org/10.1093/mnras/stx1905.

Graczyk, D., Pietrzyński, G., Thompson, I. B., et al. 2014, *ApJ*, *780*, 59. https://doi.org/10.1088/0004-637X/780/1/59.

Green, D. A., 2019, *arXiv e-prints*, arXiv:1907.02638.

Gvaramadze, V. V., Kniazev, A. Y., & Oskinova, L. M. 2019, *Mon. Not. R. Astron. Soc.*, *485*(1), L6. https://doi.org/10.1093/mnrasl/slz018.

Haberl, F., & Pietsch, W. 1999, *A&AS*, *139*, 277–. Retrieved from. http://adsabs.harvard.edu/cgi-bin/nph-bib_query?bibcode=1999A%26AS..139..277H&db_key=AST.

Haberl, F., Sturm, R., Ballet, J., et al. 2012a, *A&A*, *545*, A128. https://doi.org/10.1051/0004-6361/201219758.

Haberl, F., Sturm, R., Filipović, M. D., Pietsch, W., & Crawford, E. J. 2012b, *A&A*, *537*, L1. https://doi.org/10.1051/0004-6361/201118369.

Iyudin, A. F., Diehl, R., Bloemen, H., et al. 1994, *A&A*, *284*, L1.

Kahabka, P., Pietsch, W., Filipović, M. D., & Haberl, F. 1999, *Astron. Astrophys. Suppl. Ser.*, *136*, 81. https://doi.org/10.1051/aas:1999199.

Kavanagh, P. J., Sasaki, M., Points, S. D., et al. 2013, *A&A*, *549*, A99. https://doi.org/10.1051/0004-6361/201220431.

Kavanagh, P. J., Sasaki, M., Bozzetto, L. M., et al. 2015, *A&A*, *583*, A121. https://doi.org/10.1051/0004-6361/201526987.

Kavanagh, P. J., Sasaki, M., Bozzetto, L. M., et al. 2016, *A&A*, *586*, A4. https://doi.org/10.1051/0004-6361/201527414.

Lee, J. H., & Lee, M. G. 2014a, *ApJ*, *786*, 130. https://doi.org/10.1088/0004-637X/786/2/130.

Lee, J. H., & Lee, M. G. 2014b, *ApJ*, *793*(2), 134. https://doi.org/10.1088/0004-637X/793/2/134.

Long, K. S., Blair, W. P., Winkler, P. F., et al. 2010, *ApJS*, *187*, 495. https://doi.org/10.1088/0067-0049/187/2/495.

Long, K. S., Kuntz, K. D., Blair, W. P., et al. 2014, *ApJS*, *212*(2), 21. https://doi.org/10.1088/0067-0049/212/2/21.

Maggi, P., Haberl, F., Kavanagh, P. J., et al. 2014, *A&A*, *561*, A76. https://doi.org/10.1051/0004-6361/201322820.

Maggi, P., Haberl, F., Kavanagh, P. J., et al. 2016, *A&A*, *585*, A162. https://doi.org/10.1051/0004-6361/201526932.

Maggi, P., Filipović, M. D., Vukotić, B., et al. 2019, *A&A*, *631*, A127. https://doi.org/10.1051/0004-6361/201936583.

Massey, P., Hodge, P. W., Holmes, S., et al. 2002, *Bull. Am. Astron. Soc.*, *34*, 1272.

Mathewson, D. S., & Clarke, J. N. 1973, *ApJ*, *180*, 725. https://doi.org/10.1086/152002.

Mathewson, D. S., & Healey, J. R. 1963, *Nature*, *199*(4894), 681. https://doi.org/10.1038/199681a0.

Merloni, A., Predehl, P., Becker, W. et al., 2012, *ArXiv e-prints*.

Mochizuki, Y., Takahashi, K., Janka, H. T., Hillebrandt, W., & Diehl, R. 1999, *A&A*, *346*, 831.

Oliva, E., Moorwood, A. F. M., & Danziger, I. J. 1989, *A&A*, *214*, 307.

Sasaki, M., Gaetz, T. J., Blair, W. P., Edgar, R. J., Morse, J. A., Plucinsky, P. P., & Smith, R. K. 2006, *ApJ*, *642*, 260. https://doi.org/10.1086/500789.

Sasaki, M., Pietsch, W., Haberl, F., et al. 2012, *A&A*, *544*, 144. https://doi.org/10.1051/0004-6361/201219025.

Sasaki, M., Haberl, F., Henze, M., et al. 2018, *A&A*, *620*, A28. https://doi.org/10.1051/0004-6361/201833588.

Seward, F. D., Charles, P. A., Foster, D. L., et al. 2012, *Astrophys. J.*, *759*(2), 123. https://doi.org/10.1088/0004-637X/759/2/123.

Stiele, H., Pietsch, W., Haberl, F., et al. 2011, *A&A*, *534*, A55. https://doi.org/10.1051/0004-6361/201015270.

Vink, J. 2012, *A&A Rev.*, *20*, 49. https://doi.org/10.1007/s00159-011-0049-1.

Westerlund, B. E., & Mathewson, D. S. 1966, *MNRAS*, *131*, 371. https://doi.org/10.1093/mnras/131.3.371.

White, R. L., Long, K. S., Becker, R. H., Blair, W. P., Helfand, D. J., & Winkler, P. F. 2019, *ApJS*, *241*(2), 37. https://doi.org/10.3847/1538-4365/ab0e89.

AUTHOR BIOGRAPHY

Manami Sasaki is a Professor at Dr. Karl Remeis Observatory, which is the Astronomy Institute of Friedrich Alexander University Erlangen-Nürnberg in Germany. Remeis Observatory is part of the Erlangen Centre for Astroparticle Physics. Dr. Sasaki is a member of the German Astronomical Society, American Astronomical Society, and the International Astronomical Union. Her research focusses on multi-wavelength studies of the interstellar medium and source populations in the Milky Way and nearby galaxies. In particular, she studies the interplay of different phases of the interstellar medium, stellarend points, and star formation.

How to cite this article: Sasaki M. Supernova remnants in nearby galaxies. *Astron. Nachr*. 2020;341:156–162. https://doi.org/10.1002/asna.202023772